



Georgian bentonite clay–polymer system as a carrier for volatile oil in topical applications

LIA TSIKLAURI^{1*}, ANA JANEZASHVILI¹ and MALKHAZ GETIA²

¹Department of Technology of Pharmaceutical Products, Biologically Active Additives & Cosmetics, Iovel Kutateladze Institute of Pharmacochemistry, Tbilisi State Medical University, Tbilisi, Georgia and ²Department of Pharmaceutical Analysis & Standardization, Iovel Kutateladze Institute of Pharmacochemistry, Tbilisi State Medical University, Tbilisi, Georgia

(Received 13 May, Revised 18 July, Accepted 25 November 2025)

Abstract: This study focuses on developing a polymer–clay hybrid system using a Georgian bentonite clay (Tikha-Ascane, TA) and Carbopol (CA) as a carrier for an essential oil (EO) derived from *Matricaria chamomilla* L. cultivated in East Georgia. EO was extracted *via* hydro distillation and characterized using GC–MS and FTIR techniques. The CA–TA and CA–TA–EO formulations were evaluated for key physicochemical parameters including pH, viscosity, rheology, spreadability, compatibility, moisture loss, uniformity and stability. The EO yield was 0.3 % from air-dried plant material. The main components were bisabolol oxide A (38.2 %), α -bisabolol oxide B (12.91 %), (c*is*)- β -farnesene (11.8 %), α -bisabolol (8.83 %), spathulenol (2.27 %), chamazulene (1.99 %), *cis*-ene-yne-dicycloether (6.51 %) and β -copaene (0.38 %). These results suggest that the local chamomile chemotype is rich in bisabolol oxide A. The optimized hydrogel formulation was homogeneous, stable and demonstrated favorable rheological properties, making it suitable for topical application. Chromatographic analysis confirmed the successful incorporation of the EO into the gel, which achieved an encapsulation efficiency of 58.34 %. Overall, the study confirms the compatibility of Georgian bentonite clay with the CA polymer, forming an effective matrix for volatile oil delivery in semisolid dosage forms.

Keywords: *Matricaria chamomilla*; Tikha-Ascane; essential oil–bentonite hybrid

INTRODUCTION

Essential oils (EOs), which are complex mixtures of volatile compounds, possess numerous bioactivities and have potential applications in several industries such as the pharmaceutical, cosmetics and medicine industries. The content and chemical composition of EO are different and depend on many factors such as

* Corresponding author E-mail: l.tsiklauri@tsmu.edu
<https://doi.org/10.2298/JSC250513086T>

geographical locations, climate, the season of sampling and the method of extraction.¹ *Matricaria chamomilla* EO (MEO) exhibits strong anti-inflammatory, anti-oxidant, antimicrobial and antiviral properties and is classified as generally recognized as safe (GRAS) by the FDA.² It is widely utilized to treat various bacterial skin infections. However, its high volatility and instability, necessitate a delivery approach that improves stability and minimizes rapid evaporation to preserve its therapeutic benefits.^{3–5}

One potential solution to this issue is the encapsulation of essential oils within inorganic matrices, such as clay minerals. Clays, like bentonite are widely used as pharmaceutical ingredients or carriers due to their biocompatibility, interlayer spacing, thermal and chemical stability. The high specific surface area, excellent ion-exchange capacity, natural abundance and cost-effectiveness of bentonites make them efficient carriers for volatile oils. Loading EOs into the silicate, lowers the evaporation rate or slows the mass transfer of volatile components to the external environment. Encapsulating various types of EOs into bentonite is an efficient way to prepare novel hybrids with antifungal and antibacterial properties. Numerous studies have focused on developing EO–bentonite composites using a variety of essential oils. The use of these clays as delivery systems for essential oils represents a novel and promising approach.^{4,6}

Over recent years, polymer–clay hybrid materials have been widely utilized in drug delivery systems due to their enhanced technological properties, including rheology and drug incorporation efficiency. These materials combine the advantages of both components, such as swelling, water absorption and bioadhesion.⁷ In addition, polymer-based topical hydrogels are a promising drug delivery system for hydrophobic compounds.⁸

In this study, we describe for the first time the synthesis of a Carbopol based gel with EO obtained from *M. chamomilla* L. cultivated in Georgia and intercalated in Tikha-Ascane (TA). TA is a Georgian bentonite clay preparation obtained from the Askana Deposit (Ozurgeti region, Georgia) and investigated at the I. Kutateladze Institute of Pharmacochemistry (TSMU). The biomedical and pharmaceutical applications of TA have been approved by national public health authorities. Based on this preparation, various dermatological formulations have been developed at the Institute of Pharmacochemistry (TSMU).^{9,10}

EXPERIMENTAL

Preparation

Tikha-Ascane (TA), obtained from Georgian bentonite clay, was available at the Pharmaceutical Technology Direction (I. Kutateladze Institute of Pharmacochemistry, TSMU). Carbopol 940 (CA) and methanol (catalogue no. 34860) were purchased from Sigma–Aldrich; *n*-hexane was obtained from Carl Roth (Karlsruhe, Germany), and calcium chloride anhydrous granules were supplied by Merck. All other solvents and chemicals obtained from commercial sources were of analytical grade.

Plant material

Matricaria chamomilla L. aerial parts, cultivated in Shiraki (41°17'38" N, 46° 20'27" E, 595 m asl Kiziki Floristic Region, Georgia) were collected in early June. An 120 g air-dried sample was crushed and hydrodistilled for 2 h (1:5 herb-to-water ratio) using a Clevenger-type apparatus. The resulting dark blue essential oil with a distinct aroma was stored at 4–5 °C until analysis.

Qualitative and quantitative analysis of essential oil

MEO constituents were analyzed using an Agilent GC–MS system (GC 7890B with 5977A mass detector) equipped with an HP-5MS UI column (30 m×0.25 mm i.d.; film thickness 0.25 µm). A 1 µL sample (1:100 by volume in hexane) was injected with a split ratio of 1:150, using helium as the carrier gas (1 mL/min flow, 3 mL/min purge). The oven was programmed from 140 to 215 °C at 3 °C/min, held for 4 min; injection temperature was 250 °C. MS detection was performed in TIC and SIM modes (70 eV, 40–550 amu). The relative content of each compound was expressed as a percentage of the total chromatographic area, based on the mean of three replicates. Identification was performed by comparing retention times and mass spectra with the NIST database.¹¹

Characterization of MEO

MEO volatility was evaluated by exposing a specified quantity to the laboratory environment (room temperature, 55±5 % RH), with weight loss assessed at 3, 24, 48 and 120 h.¹¹

Preparation of gel base and formulation

The CA–TA gel base was prepared using 1.5 mass % CA and 2 mass % bentonite in an optimized 80:20 ratio. A 1% concentration of essential oil was selected based on prior data, yielding hydrogels with desirable rheological properties, stability and ease of application.¹³ To prepare the gel, 2 g of bentonite was dispersed in 4 mL of deionized water, followed by incorporation of MEO. With continuous stirring, the remaining water was gradually added and the MEO loaded clay dispersion was mixed with the 1.5 % CA gel to obtain the final hydrogel.

Characterization of formulations

Physical appearance and homogeneity were evaluated through visual inspection.¹⁴

pH Determination

The pH of all samples was determined at room temperature using a digital pH-meter (model MW150 MAX) immediately after preparation and during stability studies. The electrode was immersed into the undiluted formulations for 2 min, and the readings were recorded in triplicate.¹³

Viscosity measurement and rheological properties

A rotational viscometer (Brookfield viscometer) was used to determine the viscosity of the samples at 25±2 °C with a spindle speed of 10 rpm. The rheograms were evaluated by plotting the obtained values of shear stress *versus* shear rate.¹⁴

Determination of spreadability

The spreadability of the samples was evaluated using two sets of glass slides (20 cm×20 cm). 0.5 g of the formulations were weighed and placed within a circle of 1 cm diameter pre-marked on a glass slide. A second glass plate was positioned on it, forming a sandwich arrangement. A weight of 500 g was placed on the upper plate for about 5 min and diameters of spread circles were assessed.

The spreadability index (Si) was calculated using Eq. (1); results were obtained in relation to applied mass and spreading area:¹⁵

$$Si = d^2 \frac{\pi}{4} \quad (1)$$

where d is diameter (mm).

The spreadability factor (Sf) was calculated as:

$$Sf = \frac{A}{W} \quad (2)$$

where A is the total area (mm^2) and W is the total weight (g).

FTIR spectroscopy

FTIR analysis was conducted to inspect the compatibility of active components with excipients. Spectra of MEO, TA and Carbopol 940 were recorded for both unloaded and loaded gel formulations in the 400–4000 cm^{-1} range using a Jasco 600-IR spectrometer with a deuterated triglycine sulphate (DTGS) detector and KBr beam splitter. The essential oil was equilibrated at ambient temperature before analysis, and the resulting spectra were used as spectral fingerprints.

Determination of MEO content

Before GC–MS analysis, the samples were pretreated as follows: 0.1 g of CA–TA–MEO gel or 2.5 μg of MEO was mixed with methanol, filtered through a 0.45 μm filter, and 5 μL of the resulting solution was injected into the GC inlet *via* a split/splitless injector.

Moisture loss

The accurately weighed samples (2 g) were kept in closed desiccators containing anhydrous calcium chloride and reweighed after three days.¹² The percentage moisture loss was assessed using the following equation:

$$W = 100 \frac{W_0 - W_1}{W_0} \quad (3)$$

where W_0 is initial weight (g) and W_1 is final weight (g).

Optical microscopy

Light microscopy was used to study the microscopic characteristics of the optimized formulations. Samples were placed onto a microscopic slide and uniformly spread with a coverslip. The coverslipped slides were observed at room temperature under an optical microscope (Carl Zeiss Jena CF250) at 350 \times magnification and photomicrographs were captured on a laboratory PC.¹²

Centrifugation test

The centrifugation test was carried out to evaluate phase separation. A 2 g sample was spun at 5000 rpm for 10 min at room temperature in a 15 mL tube.

Statistical analysis

All analyses were performed in triplicate, and the means and standard deviations of the experimental data were calculated using Microsoft Office Excel.

RESULTS AND DISCUSSION

Composition of essential oil

The average yield of the oil from the dry chamomile aerial parts was calculated as 0.3 %. The components in the oil were examined using instrumental conditions

set on the GC-MS and identified using direct mass spectral comparison. The qualitative and quantitative characteristics of MEO evaluated by the GC-MS analysis are depicted in Fig. 1.

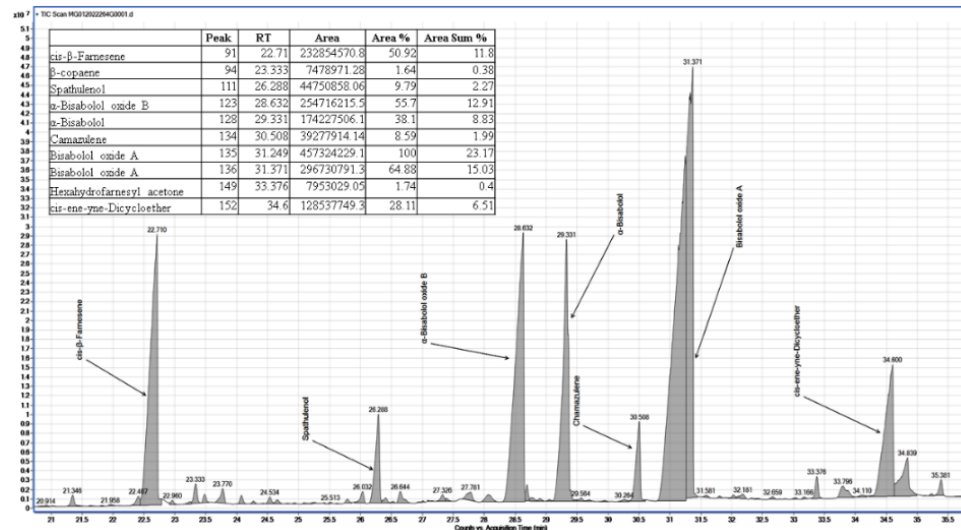


Fig. 1. GC-MS profile of essential oil extracted from dried chamomile aerial parts.

The major constituents were found to be bisabolol oxide A (38.2 %), α -bisabolol oxide B (12.91 %), (cis)- β -farnesene (11.8 %), α -bisabolol (8.83 %), spathulenol (2.27 %), chamazulene (1.99 %), cis-ene-yne-dicycloether (6.51 %) and β -copaene (0.38 %). These findings classify the East Georgian chamomile oil as a bisabolol oxide A chemotype. Bisabolol oxide A, a sesquiterpenoid, is recognized for its broad spectrum of biological activities, including anti-herpetic, antipruritic, antimicrobial, cytotoxic and antileishmanial effects.¹⁶

FTIR analysis

Essential oils are complex mixtures comprising volatile and aromatic compounds, often associated with a wide range of functional groups. In the present study, MEO was found to contain ethers, amines, carboxylic acid, aromatics, alkanes, aldehyde carbonyl, aldehyde and alcohols (Fig. 2). The assignments of corresponding functional groups were achieved by using frequency data available in the literature.¹⁷⁻¹⁹

The FTIR spectrum of MEO showed characteristic bands corresponding to its main components. A broad band at 3200–3600 cm^{-1} indicated O–H stretching from alcohols and phenols.^{18,19} A peak at $\sim 2926.45 \text{ cm}^{-1}$ was assigned to C–H stretching in alkanes.^{17,20} The band at $\sim 1717 \text{ cm}^{-1}$ was assigned to the C=O stretch

of matricin, with low intensity suggesting its conversion to chamazulene and carboxylic derivatives.^{21,22} Peaks at ~ 1631 and 1660.41 cm^{-1} indicated C=C stretching of alkenes (e.g., farnesene), while that at $\sim 1579\text{ cm}^{-1}$ was assigned to aromatic C=C vibration.^{19,27,22-25}

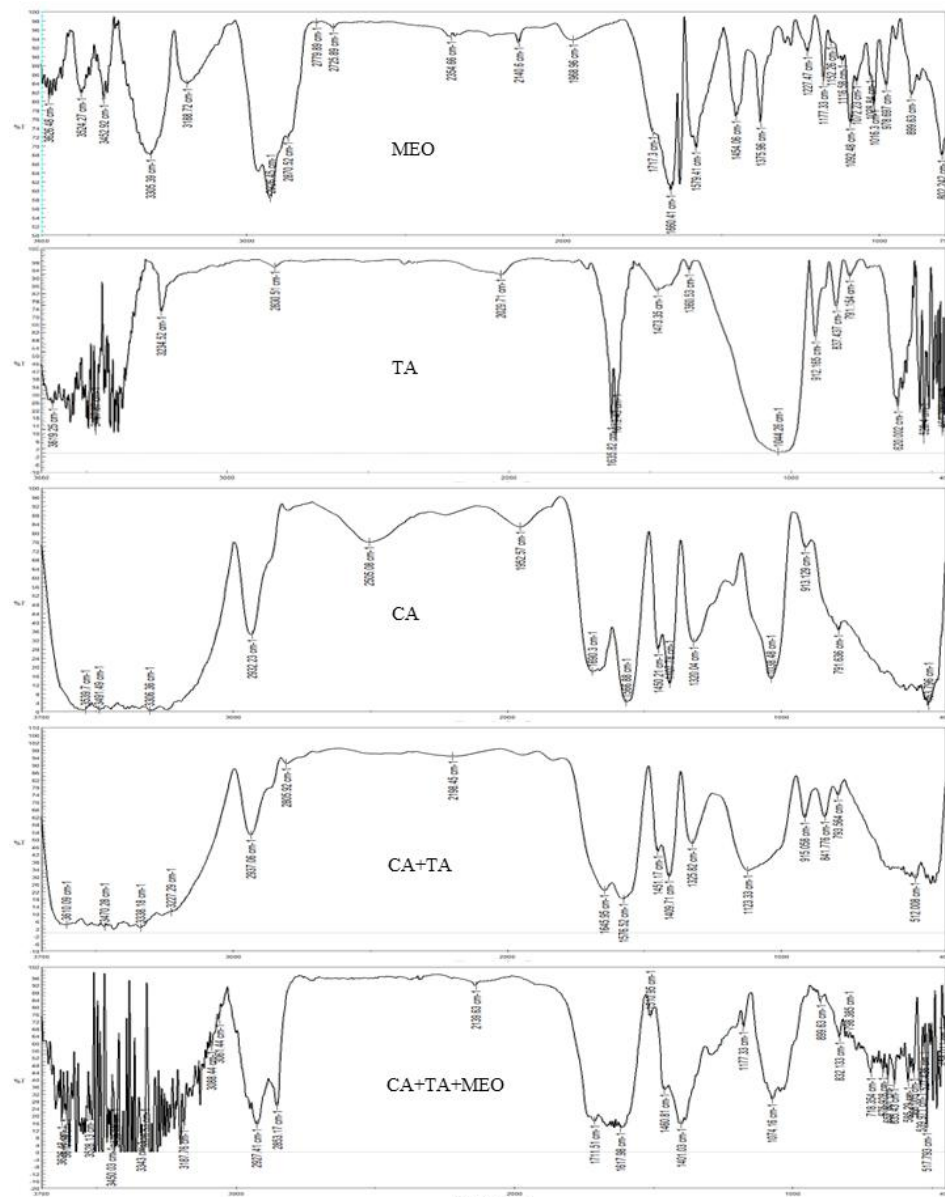


Fig. 2. FTIR spectra of the tested samples.

Bands at ~ 1454 and 1375 cm^{-1} reflected CH_2 and CH_3 deformation, possibly from α -bisabolol and its oxides.^{19,22–25} A peak around 1227 cm^{-1} corresponded to esters and phenolic C–O stretching.²⁴ Bands between 1177 – 1016.3 cm^{-1} corresponded to alcohol or ether C–O stretches, including signals from *cis/trans*-en-yne-dicycloether.^{23,24} Peaks in the 1092 – 899 cm^{-1} range matched α -bisabolol (tertiary alcohols) while the peak at $\sim 978\text{ cm}^{-1}$ indicated methylene or aromatic in-plane bending.^{19,21,23,25} Finally, peaks between 899 – 802 cm^{-1} were attributed to out-of-plane aromatic C–H bending.^{21,24}

The volatilization test revealed that free MEO exhibited weight losses of 20.3, 50.8, 53.0 and 54.7 % after 3, 24, 48 and 120 h, respectively, confirming its high volatility and highlighting the limitations of conventional encapsulation strategies. Bentonite clays, due to their unique layered structure, can effectively interact with essential oil molecules.²⁶ In this study, the interlayer space of bentonite was activated in water, followed by mechanical intercalation of MEO. This approach enabled successful incorporation of oil into the clay framework, as confirmed by volatilization assays and light microscopy (Fig. 3). Encapsulation of MEO within the bentonite matrix reduced its volatilization by 65.26, 65.32, 68.68 and 68.94 % at 3, 24, 48 and 120 h, respectively, compared to the free, unencapsulated oil, thereby demonstrating enhanced stability and decreased volatility.

As visualized in Fig. 3C, dark, spherical droplets of MEO are distributed throughout the well-dispersed carbopol–bentonite matrix, and the network structure of the hydrogel is capable of protecting the essential oil from evaporating. After addition of *Matricaria chamomilla* EO, the structure of CA–TA system changed, showing a fibrous-like network, which can be expected as a result of the interactions of matrix components with MEO compounds.

Microscopic analysis of the formulations (Fig. 3) showed that the CA–TA–MEO system exhibits a nearly monodisperse microstructure with small, homogeneously dispersed oil droplets. Droplet size is known to influence the physico-chemical stability and mechanical properties of emulsion gels. Generally, smaller droplets with a narrow size distribution improve physical stability.²⁷

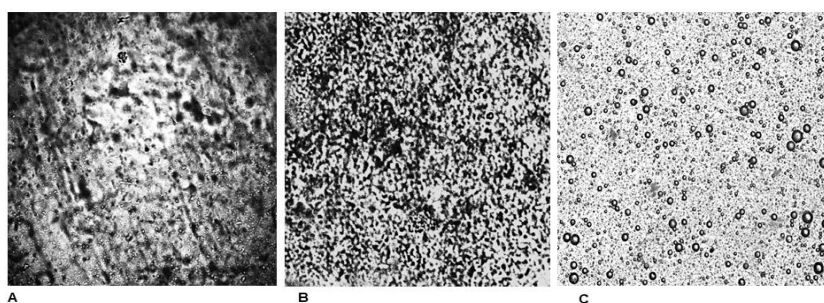


Fig. 3. Light microphotographs of tested samples. A) TA; B) CA–TA matrix; C) MEO loaded hydrogel (1 mass %).

The optical microscopy images of the hybrid microstructure of bentonite modified carbopol gel (Fig. 3B) showed a non-uniform texture. The existence of non-homogeneous areas confirms the interaction between TA and the polymer chains, providing appropriate interconnected architecture in the system. Also, Fig. 3A shows the heterogeneous texture for the aqueous TA suspension (2 mass %), typical of bentonite gels due to the clay platelets' tendency to form a structured network.

The outcome of this study showed that TA clay and the CA polymer are compatible with one another, leading to the formation of stable [TA+CA] matrix suitable for the incorporation of essential oil.

Characterization of formulations

Prepared gels were found to be blue in color, homogeneous and visually acceptable. The gel has the characteristic odor of the essential oil of *Matricaria chamomilla*.

pH Determination

The pH values of the prepared formulations are given in Table I.

The results suggest that CA-TA-MEO gel is skin-compatible and suitable for topical use.²⁸ The initial pH of bentonite suspensions ranged from 8.6 to 9.0, whereas the pH of CA-TA formulations remained between 6.5 and 6.71, and that of carbopol gels ranged from 6.47 to 6.63.

TABLE I. pH, spreadability and moisture loss of the formulations; *SD*: standard deviation, *n* = 3

Sample	pH (mean \pm SD)	<i>Sf</i> / mm ² g ⁻¹ (mean \pm SD)	<i>w</i> / %
2 % TA	8.84 \pm 0.12	—	—
1.5 % CA 940	6.53 \pm 0.06	6.89 \pm 0.52	3.33 \pm 0.05
CA-TA	6.58 \pm 0.09	6.39 \pm 0.52	4.59 \pm 0.04
CA-TA-MEO	6.57 \pm 0.04	7.16 \pm 0.33	3.76 \pm 0.03

Viscosity measurement and determination of rheological properties

The viscosity and rheology of semisolid formulations influence their application behavior and spreadability. The highest viscosity was observed for the bentonite-modified carbopol gel (78,933 cP), while the MEO gel possessed the lowest viscosity (52,267 cP). Bentonite increased the viscosity, whereas MEO incorporation into the CA-TA matrix resulted in a decrease (Fig. 4A).

The viscosity of the CA-TA-MEO gel was assessed at different speed rates; the rheological profile of formulation demonstrated a shear-thinning behavior, where viscosity decreased with increasing shear rate – indicative of a non-Newtonian, pseudoplastic system (Fig. 4C and D).

This property is advantageous for topical applications, as it enables reduced resistance during spreading while maintaining structural integrity at rest. The MEO

gel also displayed an insignificant hysteresis loop, indicating negligible thixotropic properties, a typical feature of carbomer-based gels. Such behavior enhances application consistency and storage stability.^{29,30}

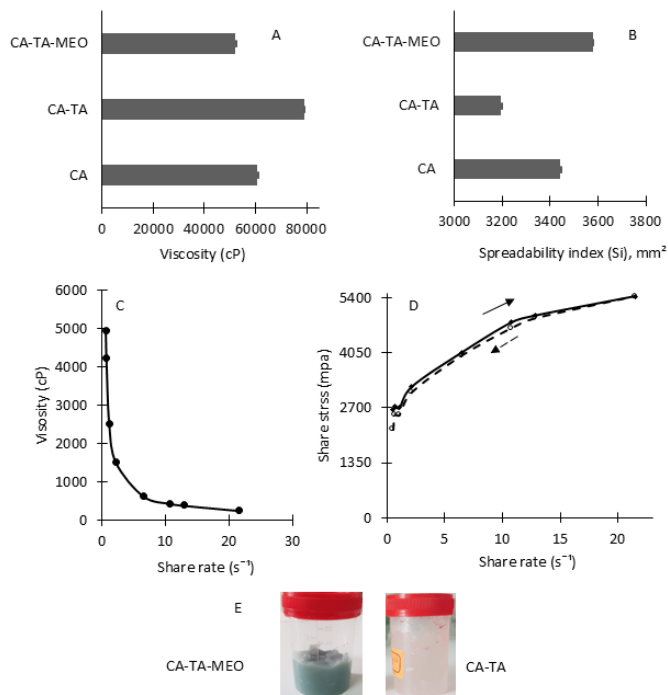


Fig. 4. Evaluation of physical properties and rheological behavior of samples: A) viscosity, B) spreadability measurements, C) viscosity at different shear rates, D) flow profile of CA-TA-EO gel and E) visual presentation of CA-TA and CA-TA-EO formulations.

Determination of spreadability

The effectiveness of topical formulations relies on uniform spreading to ensure accurate dosing and ease of application. Spreadability, a key parameter for semisolid dosage forms, is inversely related to viscosity – a decrease in viscosity leads to improved spreadability. A good spreadability for gel formulations is considered to lie within the 2500–4900 mm² range.³¹ As shown in fig. 4B and Table I, the CA-TA-MEO gel, with the lowest viscosity, exhibited the highest spreadability index (3579.21 mm²) and factor, indicating favorable spreading properties suitable for topical use.

FTIR analysis of samples

Infrared spectra of the optimized formulation confirmed the absence of incompatibility among the components. FTIR analysis also contributed to verify the pre-

sence of MEO within the TA-CA gel matrix. Similar to the spectra of CA and TA-CA, the TA-CA-MEO formulation exhibited the characteristic absorption bands of pure CA and TA-CA. The encapsulation of the essential oil by the TA-CA matrix could be evidenced by the appearance of additional specific bands corresponding to components present in MEO (Fig. 2). Bands at 2927.41 and 2853.17 cm^{-1} characteristic of the C-H stretching vibrations of alkanes, were displayed only in the TA-CA-MEO gel. Moreover, absorption peaks at \sim 1700, 1177 and 899 cm^{-1} in Fig. 2 corresponded to the C=O, stretching of aldehydes, C–O stretching of ethers, and C–H bending of aromatic compounds, respectively.²²

In the infrared spectrum of Carbopol 940 the characteristic peaks of O–H stretch at 3306.36 cm^{-1} and C–O stretch at 1407.78 cm^{-1} were observed; the peak at 2932.23 cm^{-1} represents CH_2 stretching, whereas the 1450.21 cm^{-1} peak shows the presence of the acrylate back bone (Fig. 2). It is also noted that similar peaks were found in the spectra of the hybrid matrix and TA-CA-MEO gel, confirming the structural integrity of the polymer within the formulation.³²

The bonds at 3467.87 and 3620.21 cm^{-1} in the spectrum of the original TA are characteristic of Si–OH and Al–OH stretching vibrations in bentonite. A sharp peak at 1044.26 cm^{-1} is associated with Si–O stretching vibration. Compared to the original bentonite, the Si–O absorption peak shifts to a lower wavenumber in the hybrid matrix spectrum, while in the TA-CA-MEO formulation, it moves to a higher wavenumber with reduced intensity—indicating gel network formation. The small peak at 912.16 cm^{-1} is attributed to the bending vibration of –OH in Al–Al–OH, a characteristic feature of bentonite.³³ As shown in Fig. 2, the peak at 791.15 cm^{-1} represents Al–Mg–OH vibrations, while the peak at 620.00 cm^{-1} corresponds to Mg–O–Si or Fe–O–Si groups. Peaks at 528.4 and 461.38 cm^{-1} are related to Al–O and Mg–O, respectively.³⁴

FTIR spectral analysis of the essential oil, bentonite, and Carbopol 940 confirmed that the characteristic peaks of the essential oil were preserved in the gel formulation, indicating no significant interactions among the formulation components.

Determination of MEO content

GC–MS analysis revealed comparable chromatographic profiles across the tested formulations, verifying the presence of characteristic constituents of *M. chamomilla* EO (Fig. 5). The MEO content in the CA–TA–MEO gel assessed as a function of the initial EO loading, averaged 58.34 %.

Despite the simplicity of the formulation process, a reduction in MEO content was observed, likely due to volatility or process-related factors that require further investigation. To date, no studies have reported the encapsulation efficiency of *M. chamomilla* EO in bentonite-based gels or the CA–TA system specifically. However, *EE* values for other essential oils range from 47.69 to 57.8 %, depending on

formulation variables, polymer type and analytical methods.³⁵ The *EE* observed here aligns with these findings, indicating that the CA–TA system forms a stable, well-structured matrix capable of effectively encapsulating MEO.

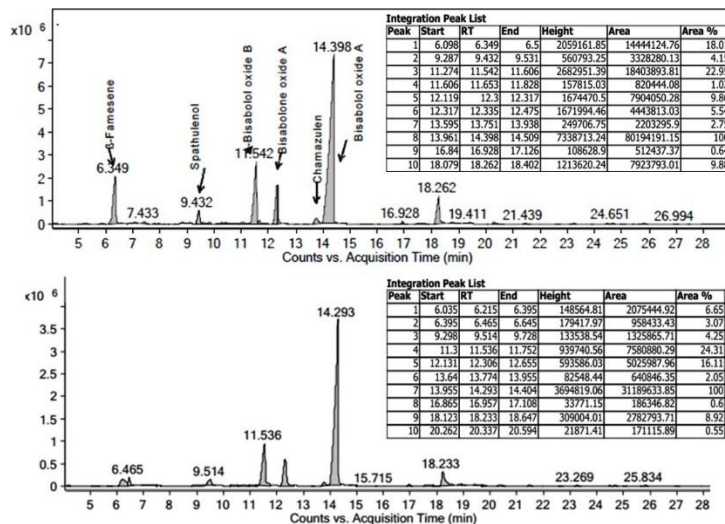


Fig. 5. GC-MS chromatograms of pure MEO (A) and CA-TA-MAO gel formulation (B).

Moisture loss

Water content is fundamental for hydrogel integrity and solubility, as evaporation significantly alters hydrogel properties.³⁶ Moisture loss analysis (Table I) showed that CA–TA–MEO exhibited the lowest loss, which is advantageous for preserving the gel's physical properties during storage. Centrifugation tests further confirmed the physical stability, with no phase separation observed.

CONCLUSION

Matricaria chamomilla essential oil (MEO) demonstrates a wide range of pharmacological activities; however, its high volatility and chemical instability hinder its direct application in topical formulations. Furthermore, MEOs compositions can vary significantly depending on factors such as geographical origin, climate, harvesting season and extraction method.

This study developed and evaluated a Georgian bentonite clay (TA)–polymer system for topical delivery of volatile oils. The gel was formulated with Carbopol (CA) and an MEO–TA hybrid. Analysis confirmed that East Georgian chamomile cultivars belong to the bisabolol oxide A chemotype, with major constituents including bisabolol oxide A, α -bisabolol oxide B, (*cis*)- β -farnesene, α -bisabolol, spathulenol, chamazulene, *cis*-ene-yne-dicycloether and β -copaene.

To minimize evaporation and slow the mass transfer of volatile components, an MEO–TA hybrid was incorporated into an 1.5 % Carbopol gel. The resulting MEO–TA–CA formulations satisfied key requirements for semisolid dosage forms, including uniformity, physical stability and suitable rheological behavior. EO droplets were well-incorporated and evenly distributed into the matrix. FTIR analysis confirmed the preservation of MEO's characteristic peaks, indicating the absence of undesirable interactions between the formulation components.

The prepared gel showed a significant encapsulation capacity for MEO, rich in bisabolol oxide A – a bioactive compound with anti-herpes, antipruritic and antimicrobial properties – highlighting the potential of Georgian bentonite clay–polymer systems for topical delivery of volatile oils.

ИЗВОД

ХИБРИДНИ СИСТЕМ ГРУЗИЈСКИ БЕНТОНИТ–ПОЛИМЕР КАО НОСАЧ ЗА ЕТЕРИЧНО УЉЕ У ТОПИКАЛНИМ ПРИМЕНАМА

LIA TSIKLAURI¹, ANA JANEZASHVILI¹ и MALKHAZ GETIA²

¹Department of Technology of Pharmaceutical Products, Biologically Active Additives & Cosmetics, Iovel Kutateladze Institute of Pharmacochemistry, Tbilisi State Medical University, Tbilisi, Georgia и ²Department of Pharmaceutical Analysis & Standardization, Iovel Kutateladze Institute of Pharmacochemistry, Tbilisi State Medical University, Tbilisi, Georgia

Циљ овог рада је био развој хибридног система полимер–глина коришћењем грузијског бентонита (*Tikha-Ascane*, TA) и полимера *Carbopol* (CA) као носача за етерично уље (EO) добијено из камилице (*Matricaria chamomilla L.*) која је узгајана у Источној Грузији. EO је екстраговано хидродестилацијом и окарактерисано применом GC–MS и FTIR техника. Одређени су основни физичко–хемијски параметри формулација CA–TA и CA–TA–EO, као што су pH, вискозност, реологија, распостирање, компатибилност, губитак влаге и стабилност. Принос EO је био 0,3 % из биљног материјала који је сушен на ваздуху. Главне компоненте су бисаболол-оксид А (38,2 %), α -бисаболол-оксид В (12,91 %), (*cis*)- β -фарнесен (11,8 %), α -бисаболол (8,83 %), спатуленол (2,27 %), камазулен (1,99 %), *cis*-ен-ин-дициклотетар (6,51 %) и β -копаен (0,38 %). Ови резултати су показали да је локална камилица богата бисаболол-оксидом А. Оптимизована хидрогел формулација је била хомогена, стабилна, са добним реолошким својствима, погодна за актуелне примене. Хроматографска анализа је потврдила успешно инкорпорирање EO у гел, са ефикасношћу имобилизације од 58,34 %. Генерално, ова испитивања су показала да је грузијски бентонит компатибилисан са CA полимером и да формира ефикасну матрицу за испоруку етеричног уља у получврстом облику.

(Примљено 13. маја, ревидирано 18. јула, прихваћено 25. новембра 2025)

REFERENCES

1. D. P. de Sousa, R. O. S. Damasceno, R. Amorati, H. A. Elshabrawy, R. D. de Castro, D. P. Bezerra, V. R. V. Nunes, R. C. Gomes, T. C. Lima, *Biomolecules* **13** (2023) 1144 (<https://doi.org/10.3390/biom13071144>)
2. A. El Mihyaoui, J. C. G. Esteves da Silva, S. Charfi, M. E. Candela Castillo, A. Lamarti, M. B. Arnao, *Life* **12** (2024) 479 (<https://doi.org/10.3390/life12040479>)

3. G. Ren, G. Ke, R. Huang, Q. Pu, J. Zhao, Q. Zheng, M. Yang, *Sci. Rep.* **12** (2022) 8153 (<https://doi.org/10.1038/s41598-022-11692-w>)
4. J. N. Saucedo-Zuñiga, S. Sánchez-Valdes, E. Ramírez-Vargas, L. Guillen, L. F. Ramos-deValle, A. Graciano-Verdugo, J. A. Uribe-Calderón, M. Valera-Zaragoza, T. Lozano-Ramírez, J. A. Rodríguez-González, J. J. Borjas-Ramos, J. D. Zuluaga-Parra, *Microporous Mesoporous Mater.* **316** (2021) 110882 (<https://doi.org/10.1016/j.micromeso.2021.110882>)
5. L. H. Oliveira, I. S. de Lima, E. R. S. da Neta, S. G. de Lima, P. Trigueiro, J. A. Osajima, E. C. da Silva-Filho, M. Jaber, M. G. Fonseca, *Appl. Clay Sci.* **245** (2023) 107158 (<https://doi.org/10.1016/j.clay.2023.107158>)
6. A. Giannakas, I. Tsagkalias, D. S. Achilias, A. Ladavos, *Appl. Clay Sci.* **146** (2017) 362 (<https://doi.org/10.1016/j.clay.2017.06.018>)
7. F. Sorouri, P. Azimzadeh Asiabi, P. Hosseini, A. Ramazani, S. Kiani, T. Akbari, M. Sharifzadeh, M. Shakoori, A. Foroumadi, L. Firoozpour, M. Amin, M. Khoobi, *Polym. Bull.* **80** (2023) 5101 (<https://doi.org/10.1007/s00289-022-04306-y>)
8. M. Chelu, *Gels* **10** (2024) 636 (<https://doi.org/10.3390/gels10100636>)
9. I. G. Kutatladze, *Tikha-Ascane for medical purpose*, Gruzmedgiz, Tbilisi, 1955, p. 40
10. L. Tsiklauri, I. Dadeshidze, G. Tsagareishvili, *Bull. Georgian Natl. Acad. Sci.* **150** (1994) 262 (ISSN 0132-1447)
11. N. Tsivelika, E. Sarrou, K. Gusheva, C. Pankou, T. Koutsos, P. Chatzopoulou, A. Mavromatis, *Biochem. Syst. Ecol.* **80** (2018) 21 (<https://doi.org/10.1016/j.bse.2018.06.001>)
12. R. Ensandoost, H. Izadi-Vasafi, H. Adelnia, *J. Macromol. Sci. Phys.* **61** (2021) 225 (<https://doi.org/10.1080/00222348.2021.1999043>)
13. N. Ullah, A. Amin, A. Farid, S. Selim, S. A. Rashid, M. I. Aziz, S. H. Kamran, M. A. Khan, N. Rahim Khan, S. Mashal, M. M. Hasan, *Gels* **9** (2023) 252 (<https://doi.org/10.3390/gels9030252>)
14. M. Singh, J. Kanoujia, P. Parashar, M. Arya, C. B. Tripathi, V. R. Sinha, S. K. Saraf, S. A. Saraf, *Drug Deliv. Transl. Res.* **8** (2018) 591 (<https://doi.org/10.1007/s13346-018-0489-5>)
15. B. Siddiqui, A. U. Rehman, I. U. Haq, N. M. Ahmad, N. Ahmed, *J. Microencapsul.* **37** (2020) 595 (<https://doi.org/10.1080/02652048.2020.1829140>)
16. I. Ikeda-Ogata, K. Yamasaki, K. Yokomizo, T. Ikeda, H. Seo, *Curr. Top. Phytochem.* **17** (2021) 63 (http://www.researchtrends.net/tia/article_pdf.asp?in=0&vn=17&tid=24&aid=6834)
17. Ö. Süfer, F. Bozok, *J. Therm. Anal. Calorim.* **140** (2020) 253 (<https://doi.org/10.1007/s10973-019-08829-x>)
18. S. Agatonovic-Kustrin, P. Ristivojevic, V. Gegechkori, T. M. Litvinova, D. W. Morton, *Appl. Sci.* **10** (2020) 7294 (<https://doi.org/10.3390/app10207294>)
19. L. Ciko, A. Andoni, F. Ylli, E. Plaku, K. Taraj, *J. Int. Environ. Appl. Sci.* **11** (2016) 154 (<https://dergipark.org.tr/tr/download/article-file/571496>)
20. M. I. Morar, F. Fetea, A. M. Rotar, M. Nagy, C. A. Semeniuc, *Bull. UASVM Food Sci. Technol.* **74** (2017) 37 (<https://doi.org/10.15835/buasvmcn-fst:12634>)
21. H. Schulz, M. Baranska, H. H. Belz, P. Rösch, M. A. Strehle, J. Popp, *Vib. Spectrosc.* **35** (2004) 81 (<https://doi.org/10.1016/j.vibspec.2003.12.014>)

22. K. Taraj, I. Malollari, A. Andoni, L. Ciko, P. Lazo, F. Ylli, A. Smeni, A. Como, *J. Environ. Prot. Ecol.* **18** (2017) 117
(<https://scibulcom.net/en/article/Sut8GqESZGR7LPJJIKEw>)
23. M. D. Berechet, E. Manaila, M. D. Stelescu, G. T. Craciun, *Rev. Chim.* **68** (2017) 2787
(<https://doi.org/10.37358/RC.17.12.5979>)
24. Y. Q. Li, D. X. Kong, H. Wu, *Ind. Crops Prod.* **41** (2013) 269
(<https://doi.org/10.1016/j.indcrop.2012.04.056>)
25. A. Andoni, F. Ylli, P. Lazo, K. Taraj, A. Como, *BSHN (UT)* **24** (2017) 152
(https://api.fshn.edu.al/uploads/1_Andoni_et_al_rreg_3bb9aef7ff.pdf)
26. L. H. de Oliveira, P. Trigueiro, J. S. N. Souza, M. S. de Carvalho, J. A. Osajima, E. C. da Silva-Filho, M. G. Fonseca, *Colloids Surfaces, B* **209** (2022) 112186
(<https://doi.org/10.1016/j.colsurfb.2021.112186>)
27. J. Santos, L. A. Trujillo-Cayado, F. Carrillo, M. L. López-Castejón, M. C. Alfaro-Rodríguez, *Polymers* **14** (2022) 2195 (<https://doi.org/10.3390/polym14112195>)
28. X. Nqoro, S. A. Adeyemi, P. Ubanako, D. T. Ndintehal, P. Kumar, Y. E. Choonara, B. A. Aderibigbe, *Polym. Bull.* **81** (2024) 3459 (<https://doi.org/10.1007/s00289-023-04879-2>)
29. M. F. A. Khan, A. Ur Rehman, H. Howari, A. Alhodaib, F. Ullah, Z. ul Mustafa, A. Elaissari, N. Ahmed, *Gels* **8** (2022) 277 (<https://doi.org/10.3390/gels8050277>)
30. Y. Maslii, O. Ruban, G. Kasparaviciene, Z. Kalveniene, A. Materiienko, L. Ivanauskas, A. Mazurkeviciute, D. M. Kopustinskiene, J. Bernatoniene, *Molecules* **25** (2020) 5018
(<https://doi.org/10.3390/molecules25215018>)
31. M. X. Chen, K. S. Alexander, G. Baki, *J. Pharm. (Cairo)* **2016** (2016) 5754349
(<https://doi.org/10.1155/2016/5754349>)
32. J. El Karkouri, M. Bouhrim, O. M. Al Kamaly, H. Mechchate, A. Kchibale, I. Adadi, S. Amine, S. Alaoui Ismaili, T. Zair, *Plants* **10** (2021) 2068
(<https://doi.org/10.3390/plants10102068>)
33. M. G. Martins, D. O. A. Martins, B. L. C. de Carvalho, L. A. Mercante, S. Soriano, M. Andruh, M. D. Vieira, M. G. F. Vaz, *J. Solid State Chem.* **228** (2015) 99
(<https://doi.org/10.1016/j.jssc.2015.04.024>)
34. M. Edraki, D. Zaarei, *J. Nanoanalysis* **5** (2018) 26
(<https://sanad.iau.ir/fa/Journal/jnanoanalysis/DownloadFile/988806>)
35. K. G. Torres, R. R. Almeida, S. Y. de Carvalho, J. F. Haddad, A. A. Leitao, L. G. Guimaraes, *Mater. Today Commun.* **24** (2020) 101252
(<https://doi.org/10.1016/j.mtcomm.2020.101252>)
36. A. Vesković, D. Nakarada, A. Popović Bijelić, *Polym. Test.* **98** (2021) 107187
(<https://doi.org/10.1016/j.polymertesting.2021.107187>).